Electrical double layer as a model of interaction between cellulose and solid acid catalysts of hydrolysis

Nikolay Tarabanko[@], Valery E. Tarabanko, Sergey V. Kukhtetskiy, Oxana P. Taran

December 7, 2018

@: Corresponding author: tarabanko.nv@icct.krasn.ru; Tel.: +07-391-205-1936
Institute of Chemistry and Chemical Technology SB RAS, Federal Research Center "Krasnoyarsk Science Center SB RAS", Akademgorodok 50/24, Krasnoyarsk 660036, Russia; chem@icct.ru

Abstract

Solid acid catalysts of cellulose hydrolysis in aqueous media attract considerable research interest because of the ease of their separation from the reaction products. The nature of interaction between the two solids is a relevant topic of ongoing research. One aspect of behavior of solid acids in water was not previously discussed in literature with regard to hydrolysis of cellulose: electrolytic dissociation and formation of electric double layers. In this work, on theoretical level, we consider the role of the double layer created by the solid acid when cellulose hydrolysis takes place. The diffuse layer of protons is regarded as the medium where the hydrolysis reaction occurs. Protonation of cellulose by these protons imparts positive charge onto its surface, and cellulose is electrostatically attracted to the polyanion of the catalyst. Thus, the two solid surfaces stay close to each other despite Brownian motion; this allows explaining the high activity of solid catalysts even when chemisorption of carbohydrates on a catalyst is not favorable.

Keywords: Acid catalysis, Cellulose hydrolysis, Electrostatic interactions, Heterogeneous catalysis, Thermodynamics

1 Introduction

Replacing fossil feedstocks used for large-scale chemical syntheses in favor of renewable organic matter is a recognized scientific and industrial priority [1]. Vast quantities of plant biomass are available at minimum expense in the form of agricultural byproducts [2]. A considerable portion of this biomass is represented by cellulose. This polymer can be hydrolyzed into soluble sugars, and the latter can be used as a feedstock for producing a multitude of chemicals: fuels like bioethanol or biobutanol, biodegradable polymer precursors like levulinic acid, platform chemicals (5hydroxymethyl furfural), etc [3, 4]. Catalysis of cellulose hydrolysis by strong mineral acids is well known and efficient, but isolation of the catalyst from the reaction products is complicated [5]. Enzyme-catalyzed hydrolysis is slow, but the products are suitable for bio-processing since they are free of acids or byproducts from acid-induced sugar conversion, which are harmful to microorganisms [6]. Ionic liquids attract research interest; one of their interesting features is the ability to break down the intermolecular hydrogen bonds in cellulose and dissolve it. Properties of ionic liquids can be widely varied: for example, they can serve as an acid catalyst [7] or facilitate enzymatic hydrolysis [8].

In 2008, possibility of cellulose hydrolysis with solid catalysts (sulfonated or oxidized carbons, ion exchange resins, zeolites, acidic oxide catalysts) was demonstrated [9, 10]. Heterogeneously catalyzed cellulose hydrolysis proceeds in quite harsh conditions (150–180 °C) [11]; however, this circumstance is also common in homogeneous acid-catalyzed processes. The clear benefit of the solid catalysts is the ease of their separation from the reaction medium: this can be made trivial by embedding magnetic particles inside catalyst grains [12]. Solid catalysts of cellulose conversion are actively developed in the direction of bifunctionality and one-pot processes combining hydrolysis and hydrogenation [13, 14, 15].

When using solid acids for cellulose hydrolysis, one should be wary of a possibility that a solid catalyst may decompose, releasing a homogeneous acid into the reaction medium, which then causes catalytic action. For example, this happens when hydrolysis of C-Cl bonds occurs in a catalyst modified with chlorine atoms, which leads to formation of hydrochloric acid [16]. On the other hand, there are numerous experimental facts which suggest quite certainly that surface-bonded acid sites can cause hydrolysis of cellulose and subsequent transformation of the soluble sugars. The catalytic action of these acid sites has considerable

differences in comparison to dissolved acids. In hydrolysis of cellulose and eucalyptus timber into glucose, sulfonated carbons exhibit higher activity per one sulfate group than homogeneous sulfuric acid under equivalent conditions [10]. In acid-catalyzed deep conversion of carbohydrates, sulfonated carbons are not only more active compared to the equivalent amount of sulfuric acid, but also change the product composition: The principal product of cellulose conversion by aqueous H_2SO_4 at temperatures up to 200 °C is levulinic acid, while sulfonated carbons mainly give 5-hydroxymethyl furfural (5-HMF) [17].

Despite continued research into hydrolysis of cellulose using solid acid catalysts over the last decade [18, 13, 19, 16, 20, 21, 22], the mechanism of the interaction between the two solid substances remains largely unclear. Initially, it was suggested that the peculiarities of the catalytic action by covalently bonded sulfonic groups on carbon surface are caused by lower solvation of the acid cites in comparison to homogeneous solution [10]. Chemisorption of β-1,4 glucan molecules was observed on a catalyst bearing sulfonic and organic acid groups, and the organic groups were identified as responsible for adsorption; whereas sulfonic groups were believed to be responsible for the actual hydrolysis reaction [10]. This specialized action of different acid groups was likened to the behavior of enzymes [23]. None of the listed statements were developed enough to offer quantitative description of the underlying physico-chemical phenomena. However, on qualitative level, there may be merit in the hypothesis about limited solvation in the catalyst vicinity. For example, this can be one of the possible reasons why 5-HMF tends to not degrade into levulinic acid under catalysis by solid acids: Transformation of 5-HMF into levulinic acid includes a hydration step [24]; thus, low activity of water in the reaction medium is a key factor of 5-HMF stability. This is why 5-HMF principally forms in non-aqueous media (polyethylene glycol [25], dimethyl sulfoxide [26], dioxane [27], etc.) or aqueous systems with lowered water activity (e.g., concentrated sodium hydrogen sulfate solution [27]).

In the discussion of the catalytic mechanism of zeolites in an ionic liquid medium ($[BMIm]^+Cl^-$), a conclusion is made that 1-butyl-3-methyl imidazolium cations are exchanged for protons in the zeolite pores, and these protons catalyze hydrolysis outside of the solid catalyst [28]. Such ion exchange may also take place in aqueous media in the presence of dissolved electrolytes. However, this exchange cannot fully explain the herein above described unique properties of solid acid catalysts.

β-1,4 glucan chains were found to be easily hydrolyzed if covalently grafted onto surfaces of silica or alumina that are rich with mildly acidic hydroxylic defects [29]. It was found that the acid site density had crucial effect on the hydrolysis rate. Hydrogen bonding of the surface acid sites to glycosidic oxygen atoms was theorized to be necessary for hydrolysis to take place [29]; the hydrolysis pathway itself was theorized to be of the general acid catalysis type (i.e., independent of the acid strength) [30]. The apparent activation energy of the described hydrolysis process was 70–87 kJ mol^{-1} [29], which is markedly lower than in hydrolysis by sulfuric acid (170 kJ mol^{-1}) [10], or a carbon with both sulfonic and organic acid sites (110 kJ mol^{-1}) [10]. However, in practice, weakly acidic inorganic materials like aluminosilicates tend to perform poorly in cellulose hydrolysis, and their catalytic activity appears to increase with the acid site strength [11], suggesting the influence of the factors other than hydrogen bonding.

Chemisorption of sugars on oxidized carbons was studied experimentally and by computational chemistry simulations [31]. Thermochemical data for Langmuir adsorption of glucose, cellobiose, and cellotriose were obtained. A conclusion was made that adsorption favors hydrophobic regions of the carbon surface. The measured chemisorption is quite strong: For example, based on the data for cellotriose [31], the adsorption free energy at 453 K would be $\Delta G_{ads} = -11.6$ kJ mol^{-1} per one glucose link. This is considerably greater by absolute value than the thermal energy at this temperature ($RT = 3.77$ kJ mol^{-1}), so it seems that adsorption of even one glucose link should result in reliable adhesion of solid cellulose to the catalyst. However, such manipulations with the thermochemical data do not appear to be sufficient to predict the behavior of solid cellulose. The oxidized carbon used for the measurement of these data was reported as unable to adsorb ball-milled cellulose at relatively low temperature 296 K [31]. On the other hand, a carbon with multiple functionalization (sulfonic, carboxylic, and phenolic) was reported to adhere to filter paper strongly enough to withstand ultrasonic cleaning [10]. Evidently, chemisorption of cellulose on solid acids is a complex subject with many as yet unknown variables, and the role of this chemisorption in hydrolysis experiments may depend on many circumstances.

In order to model the catalytic reactions on oxidized carbons, catalytic activity of various substituted benzoic acids in hydrolysis of cellobiose and cellulose was studied [32]. It was shown that the hydrolytic activity of acids does not correlate with their pK_a value, i.e., the process does not obey the patterns of specific catalysis by hydronium ions. The paper [32] revealed no notable difference in apparent hydrolysis activation energies between different studied acids (110–120 kJ mol^{-1}). However, it was shown that the frequency factor is higher for phthalic and salicylic acids because their association with carbohydrates by hydrogen bonding makes the formation of the activated complex more probable. This is a possible explanation why oxidized carbons have high hydrolytic activity despite relatively low acid strength of the active sites [32].

Such aspect of a solid acid's behavior in aqueous media as dissociation of the former and formation of an electrical double layer is to this moment not discussed in literature in the context of cellulose hydrolysis. However, consideration of this phenomenon appears to be important: existence of a diffuse proton cloud around a catalyst particle would allow extending the acid catalytic action beyond the surface of the catalyst. Another phenomenon that is worth considering here is how redistribution of charge in the system "solid acid–water–cellulose" can result in a pair of oppositely charged surfaces (positive protonated cellulose and negative dissociated catalyst) that attract to each other (Figure 1). It may seem that the positive charge of the protonated cellulose should repel the proton cloud and greatly limit its influence. But the Boltzmann distribution can lead to existence of a fraction among the protons that have sufficiently high thermal motion energy to overcome the electrostatic repulsion. The electrostatic attraction between the two solids would ensure their adherence to each other, possibly until the cellulose is completely hydrolyzed. Practically, this would mean that all the available acid groups of the catalyst are constantly "busy" hydrolyzing the cellulose via the diffuse layer, and such hydrolysis proceeds in the thin near-surface region where relatively high proton concentrations may be attained. If correct, this hypothesis is a possible explanation of the high activity exhibited by the solid acid catalysts of cellulose hydrolysis.

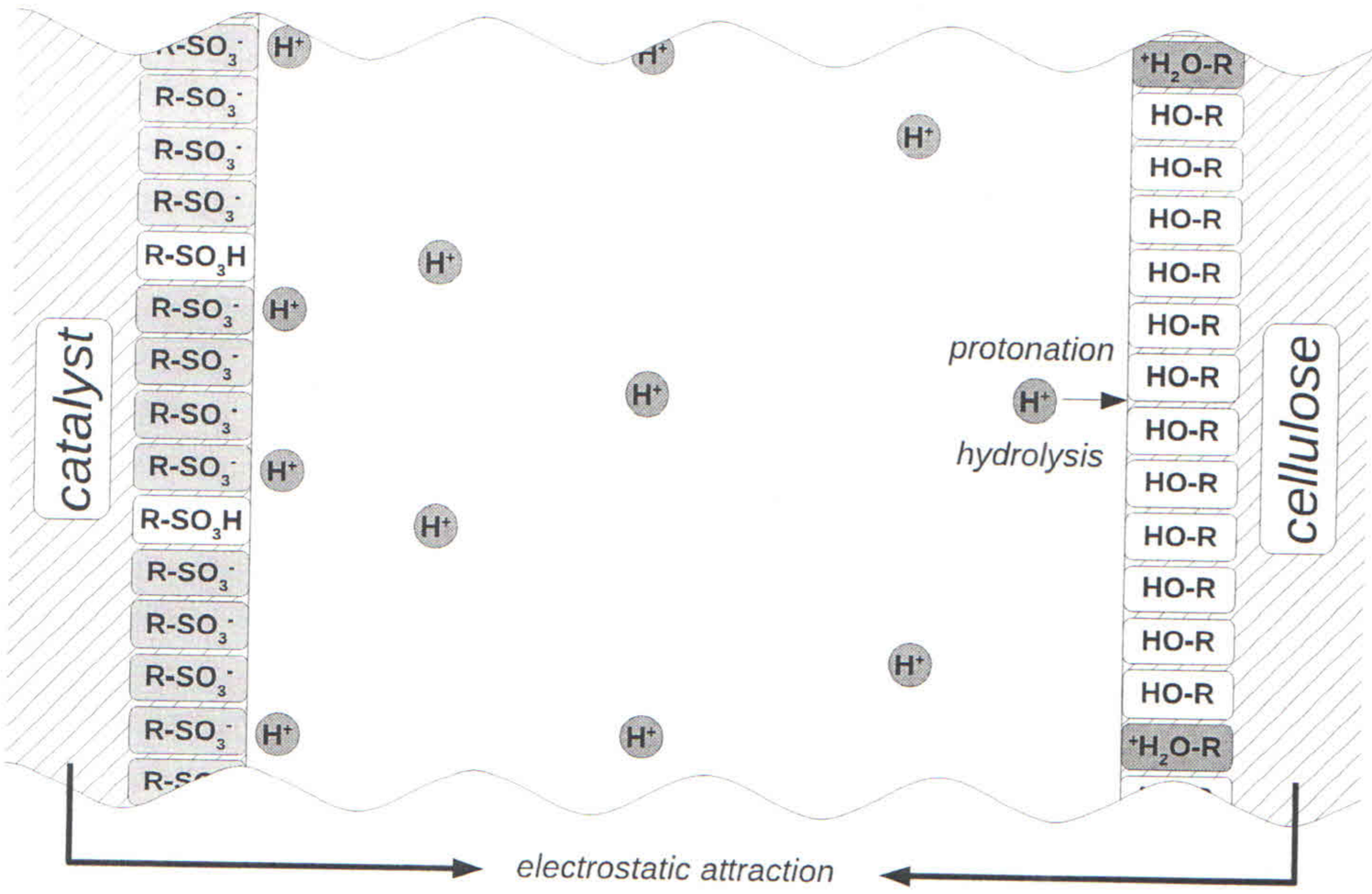

Figure 1: Schematic representation of the proposed electric double layer model for interaction of cellulose with solid acid catalysts.

In this work, we make the first attempt to describe the interaction of cellulose and solid acid catalysts of hydrolysis from the electrical double layer point of view. This is a theoretical work in which we propose a simple model that quantitatively describes the diffuse layer between the surfaces of a solid acid catalyst and cellulose in aqueous media. Specifically, we will focus on proton concentrations that are attained near the cellulose surface, and electrostatic interaction energies. This paper is structured in the following manner. In the Theoretical section, we define the model and describe the calculation procedures. In the Results section, we present the obtained data and explain the patterns observed in the presented dependences. In the Discussion section, we try to establish connection between our calculation results and literature data on various experiments with cellulose hydrolysis by solid acids.

2 Theoretical

2.1 The electrical double layer model

Extensive research has been devoted to the nature of electrical double layers in colloid chemistry and electrode phenomena [33, 34], and dissociation of flexible polymeric polyelectrolyte molecules [35, 36]. However, there are some distinguishing features of a rigid surface-functionalized polyelectrolyte (for simplicity, we will henceforth refer to it as solid acid catalyst or SAC) that sets this kind of system apart from those mainline ones. Unlike in typical colloid or electrode systems, the diffuse

electrical layer around SAC is formed by the ions from the SAC dissociation itself, and the surface charge results from the same phenomenon (rather than adsorption and attraction of ions from the background electrolyte). At the same time, thanks to the spatial rigidity, the SAC model does not require the same level of complexity as would be necessary for modeling flexible molecules.

Another thing that is necessary to include in the proposed model is the solid substrate that interacts with the acid catalyst. The concept of catalysis by dissociated acids implies protonation of the substrate in the beginning of the reaction pathway. Because our substrate is solid, such protonation creates a charged surface that affects the distribution of spatial charge.

Since the model that we propose is the first known attempt to describe the interaction of SACs with solid substrates mediated by the double layer, it appears acceptable to impose a number of simplifications. The model is based on the following postulates:

1. The interacting solids have perfectly spherical shape, and their radii are much larger than the distance between the surfaces. In this case, the interacting solids can be treated as infinitely spanning parallel flat surfaces, effectively rendering the mathematical problem unidimensional. This seems to be a reasonable approximation even where practical sizes of particles are concerned. For example, if we take a sphere of radius $r_s = 10$ μm and cut off a spherical cap with the base radius $r_c = 500$ nm, then this cap will have "thickness" $h = r_s - \sqrt{r_s^2 - r_c^2} = 12.5$ nm. This cap seems mostly flat and far-spanning when compared to inter-surface distances up to 100 nm. But then, real interacting particles very likely have not quite spherical surfaces where reasonably flat facets can be expected. Besides the obvious benefit of unidimensional mathematical simplicity, the results from this model can be extrapolated towards the force of interaction between spherical particles via the Derjaguin approximation [37]. Knowing this force will simplify calculation of the electrostatic potential energy of interaction between spherical particles at different distances.

2. The interacting surfaces are smooth and non-porous.

3. The space between the surfaces is an abstract homogeneous continuum which can be described by proton concentration C_{H+} in any point of this space. The protons and their solvated forms are considered to have no size, their charge is uniformly distributed in space yielding charge density $\rho_q = FC_{H+}$ (F is the Faraday constant). When protons associate with a surface, they are considered to just "sink" into it, imparting their charge to the surface.

4. There is acid dissociation equilibrium with said continuum at both interacting surfaces. The protons that constitute non-dissociated functional groups can be considered as a sort of specifically adsorbed electrical layer. This is the only form of trying to account for surface phenomena in this system. Even so, quantification of these equilibria is non-trivial. Ideally, this quantification should follow proton binding isotherms (dependency of dissociation ratio versus pH of the medium) that were determined experimentally. However, it appears that no such data are available in literature for sulfonated solids. This situation is further complicated by the fact that the known cellulose hydrolysis experiments take place at considerable temperatures and pressures; this means that acquisition of proton binding isotherms which adequately correspond to the hydrolysis conditions demands dedicated equipment (essentially, potentiometric titration is required [38]).
As for room temperature, a proton binding isotherm of an oxidized carbon is known [39]. This dependence corresponds to the pK_a distribution of acid sites that has a well-defined peak at pK_a 3, together with circa fourfold larger amount of acid sites around pK_a 11. The latter correspond to phenolic groups [10]. The former can be attributed to carboxylic groups in close proximity to phenolic groups (e.g., pK_a of salicylic acid is also 3 [32]). Based on this example, it would seem that despite accumulation of negative charge on the polyanion due to dissociation, the remaining non-dissociated acid groups suffer almost no acidity decrease. This is stark contrast with molecular polyprotic acids where pK_a at each subsequent dissociation step can be over a unit higher than at the previous one (e.g., in phthalic acid pK_{a_1} 2.76, pK_{a_2} 4.92 [40]). In our calculations, we assume that the entire surface of an oxidized carbon SAC can be described with pK_a 3. As for modeling of a sulfonated SAC, we will also assume equality of acidity between a solid acid and the corresponding soluble acid, specifically 4-toluenesulfonic acid with pK_a −1.34 [40]. We assume that this value describes the entire sulfonated SAC surface, whether a sulfonic ion exchange resin like Amberlyst®-15 or a sulfonated carbon, both of which are commonly tested in cellulose hydrolysis in literature. The physico-chemical meaning of the acidity constant is interpreted according to the equation:

$$K_a = \frac{[H^+_{SAC}][RSO_3^-]}{[RSO_3H]}, \tag{1}$$

where $[H^+_{SAC}]$ is the homogeneous proton thermodynamic activity (numerically equivalent to the molar proton concentration) in the interplanar space immediately adjacent to the SAC surface, $[RSO_3^-]$ and $[RSO_3H]$ are the surface activities of the dissociated and non-dissociated acid groups respectively. The latter two activities will be considered numerically

equivalent to the molar fraction of the corresponding species based on the total amount of the acid groups. So, (1) can be rewritten as:

$$K_a = C_{H^+_{SAC}} \frac{\alpha_{diss}}{1 - \alpha_{diss}}, \tag{2}$$

where $C_{H^+_{SAC}}$ is the equilibrium proton concentration near the SAC surface, and α_{diss} is the fraction of dissociated acid groups.

Quantifying the cellulose-side equilibrium is also problematic. Despite having clear relevance to the subject of hydrolysis kinetics, equilibrium of cellulose protonation appears to be unexplored. So, another approximation is necessary. Acidity of protonated alcohols R-OH_2^+ is rated at pK_c −2 [41]. This value will be considered to describe the entire cellulose surface in a fashion similar to the SAC:

$$K_c = C_{H^+_{cell}} \frac{1 - \alpha_{prot}}{\alpha_{prot}}, \tag{3}$$

where $C_{H^+_{cell}}$ is the equilibrium proton concentration near the cellulose surface, and α_{prot} is the fraction of protonated glucose links (we consider that any glucose link may be protonated only once).

5. The electric charge of the dissociated acid groups or protonated glucose links is non-localized and uniformly distributed across the corresponding surface.

6. The protons that are not associated with either of the surfaces are distributed in the interplanar space according to the Poisson-Boltzmann equation (more on this below), forming a diffuse electrical layer.

7. The dielectric constant of the space between the surfaces is equal to that of pure water [42] in any point of this space.

8. Self-ionization of water is ignored. This implies that the results from this model only make sense where the near-cellulose proton concentration in the diffuse layer is at least an order of magnitude higher than what would result from water self-ionization [42] in the absence of added acids ($2 \cdot 10^{-6}$ mol l^{-1} at 453 K).

2.2 The Poisson-Boltzmann equation

For simplicity of representation, all charge and potential values in the following formulae are considered to be non-negative (i.e., absolute values).

Considering the SAC surface as the 0 volt reference for the electric potential in the system, and noting that the space charge is determined only by the protons originating from the SAC, unidimensional Poisson-Boltzmann equation [43] can be written as:

$$\frac{d^2\varphi}{dx^2} = -\frac{1}{\varepsilon\varepsilon_0} F C_{H^+} = -\frac{1}{\varepsilon\varepsilon_0} F C_{H^+_{SAC}} \exp(-\frac{F}{RT}\varphi). \tag{4}$$

In order to maintain the overall electric neutrality in the system, one has to ensure that the positive charges in the space and on the cellulose surface are balanced by the SAC negative charge. Since $C_{H^+_{SAC}} \exp(-\varphi F/RT)$ represents proton concentration at any point in the interplanar space with the electric potential φ, then defining the x coordinate as 0 at the SAC surface, and defining distance between the surfaces as d_{ip}, we can express the space charge as:

$$\sigma_{space} = F C_{H^+_{SAC}} \int_0^{d_{ip}} \exp(-\frac{F}{RT}\varphi) dx. \tag{5}$$

σ_{space} is the planar density of the charge contained across the layer of space "sandwiched" by the solid surfaces. Defining the planar charge densities on the surfaces of the SAC and the cellulose as σ_{SAC} and σ_{cell} respectively, we can write down the expression for the electric neutrality constraint:

$$F C_{H^+_{SAC}} \int_0^{d_{ip}} \exp(-\frac{F}{RT}\varphi) dx = \sigma_{SAC} - \sigma_{cell}. \tag{6}$$

Charge densities on the solid surfaces can be calculated from the surface concentrations of the functional groups that can dissociate on the SAC (Γ_{SAC}) or glucose links that can be protonated on cellulose (Γ_{cell}). From the equations that define acid

dissociation equilibria (2),(3), it follows:

$$\sigma_{SAC} = F\Gamma_{SAC}\alpha_{diss} = F\Gamma_{SAC}\frac{K_a}{K_a + C_{H^+_{SAC}}}, \tag{7}$$

$$\sigma_{cell} = F\Gamma_{cell}\alpha_{prot} = F\Gamma_{cell}\frac{C_{H^+_{cell}}}{K_c + C_{H^+_{cell}}}, \tag{8}$$

$$C_{H^+_{cell}} = C_{H^+_{SAC}} \exp(-\frac{F}{RT}\varphi_{cell}), \tag{9}$$

where φ_{cell} is the electric potential at the cellulose surface. Based on Equations (7),(8),(9), we can rewrite Equation (6):

$$C_{H^+_{SAC}} \int_0^{d_{ip}} \exp(-\frac{F}{RT}\varphi)dx = \frac{\Gamma_{SAC}K_a}{K_a + C_{H^+_{SAC}}} - \frac{\Gamma_{cell}C_{H^+_{SAC}} \exp(-\frac{F}{RT}\varphi_{cell})}{K_c + C_{H^+_{SAC}} \exp(-\frac{F}{RT}\varphi_{cell})}. \tag{10}$$

Now, we express the near-SAC spatial charge density $\rho_{q_{SAC}}$ (11) from the electric neutrality Equation (10). $\rho_{q_{SAC}}$ is the real positive root of the cubic equation (12) with coefficients (13)-(16).

$$\rho_{q_{SAC}} = FC_{H^+_{SAC}} \tag{11}$$

$$\alpha_0 + \alpha_1\rho_{q_{SAC}} + \alpha_2\rho^2_{q_{SAC}} + \alpha_3\rho^3_{q_{SAC}} = 0 \tag{12}$$

$$\alpha_0 = F\Gamma_{SAC}K_aK_c \tag{13}$$

$$\alpha_1 = YK_a(\Gamma_{SAC} - \Gamma_{cell}) - ZK_aK_c \tag{14}$$

$$\alpha_2 = -\frac{Y(ZK_a + \Gamma_{cell}) + ZK_c}{F} \tag{15}$$

$$\alpha_3 = -\frac{YZ}{F^2} \tag{16}$$

$$Y = \exp(-\frac{F}{RT}\varphi_{cell}) \tag{17}$$

$$Z = \int_0^{d_{ip}} \exp(-\frac{F}{RT}\varphi)dx \tag{18}$$

Finally, the Poisson-Boltzmann equation (4) can be written as:

$$\frac{d^2\varphi}{dx^2} = -\frac{1}{\varepsilon\varepsilon_0}\rho_{q_{SAC}} \exp(-\frac{F}{RT}\varphi), \tag{19}$$

where $\rho_{q_{SAC}}$ is itself a function of the electric potential according to Equations (12)-(18). Although the resulting Poisson-Boltzmann equation is quite complex, it inherently accounts for the dissociation equilibria near the solid surfaces. So, finding the equilibrium distribution of charge in the system only requires solving (19) for φ values, which can be done iteratively as described in Section 2.3. The boundary values for this problem are these:

$$\varphi|_{x=0} = 0, \tag{20}$$

$$\left.\frac{d\varphi}{dx}\right|_{x=d_{ip}} = \frac{\Gamma_{cell}\rho_{q_{SAC}}Y}{\varepsilon\varepsilon_0(K_c + \frac{\rho_{q_{SAC}}Y}{F})}. \tag{21}$$

The former boundary value (20) defines the zero reference for the electric potential. The latter value (21) arises from the relations between charge, potential, and electric field strength. Noting that the surfaces are considered infinitely spanning and parallel, electric field strength at any point between them—or rather at any point on a plane that is at the given distance from the SAC and parallel to the charged surfaces—only depends on how much charge is on either side of the plane in question. Also considering

how electric field is a derivative of potential, we obtain:

$$\left.\frac{d\varphi}{dx}\right|_{x=d_{ip}} = E_{x=d_{ip}} = \frac{\sigma_{cell}}{\varepsilon\varepsilon_0}. \tag{22}$$

Ordinarily, a charged plane creates a field of $\sigma/2\varepsilon\varepsilon_0$ in front of it (as per the Gauss-Ostrogradsky theorem [44]). However, at any point (plane) between the surfaces, there are opposite charges of equal absolute value on both sides of such plane (as dictated by the charge conservation law), and the interplanar electric field is thus doubled. To express σ in familiar terms, Equations (9),(17) are plugged into (8), the resulting σ_{cell} is expressed in terms of $\rho_{q_{SAC}}$ as per Equation (11). Finally, Equation (21) is obtained.

2.3 The calculation procedure

The following parameters are used in the calculation:

- Γ_{SAC}—surface concentration of acid groups on the solid acid catalyst. In experiments, this typically measures around 1–2 μmol m^{-2} (approximated as the quotient of measured acid group amount and specific surface area) [9, 17, 11].
- Γ_{cell}—surface concentration of glucose links on the cellulose surface. We will use a conservative value 1.94 μmol m^{-2}which corresponds to the (110) surface—the one with the lowest Γ_{cell}—of the I_α polymorph [45].
- K_a and K_c—acidity constants for the SAC acid groups and protonated glucose links respectively. These were discussed in detail in Section 2.1.
- r—radius of the SAC and cellulose particles. For simplicity, we consider that they have the same size.
- ρ_{SAC}—density of the SAC particles. Considered equal to wetted particle density of activated carbon, 1200 kg m^{-3} [46].
- ρ_{cell}—density of wetted cellulose particles, 1600 kg m^{-3} [47].

The electrical double layer configuration and the particle interaction force are calculated according to the following procedure:

1. Assign N (typically 301) evenly spaced points along the interplanar distance. The first point is 0 (located on the SAC surface), the last one is d_{ip} (on the cellulose surface).
2. Make an educated initial guess about the potential values $\varphi_{i(in)}$ at all assigned points in the space ($i = 1, \ldots, N$).
3. This step calculates the potential values φ_i for the N space points that satisfy the Poisson-Boltzmann equation (19) and the boundary conditions (20), (21). This is done via the finite difference method [48]. Discretization of Equations (19),(20),(21) leads to a new system of equations:

$$\varphi_1 = 0, \tag{23}$$

$$\frac{1}{\Delta x}(\varphi_N - \varphi_{N-1}) = \frac{\Gamma_{cell}\rho_{q_{SAC}}Y}{\varepsilon\varepsilon_0(K_c + \frac{\rho_{q_{SAC}}Y}{F})}. \tag{24}$$

$$\frac{1}{\Delta x^2}(\varphi_{i-1} - 2\varphi_i + \varphi_{i+1}) = -\frac{1}{\varepsilon\varepsilon_0}\rho_{q_{SAC}}\exp(-\frac{F}{RT}\varphi_i),\ i = 2, \ldots, N-1, \tag{25}$$

where $\Delta x = d_{ip}/(N-1)$ is the integration step; while Y, Z, and $\rho_{q_{SAC}}$ are defined by Equations (17), (18), and (12), respectively. Equations (23),(24) are the boundary conditions, and (25) represents the finite difference expressions. Iterative solution is employed.

   (a) Calculate the Y and Z values (17),(18) based on $\varphi_{i(in)}$ (integration is accomplished using *SciPy integrate.trapz* routine [49]). Calculate $\rho_{q_{SAC}}$ as the only real positive root of the equation (12), as found by using *NumPy roots* routine [49].

   (b) Expressions (25) are linearized by reassigning the exponential terms as constants $L_i = \exp(-\varphi_{i(in)}F/RT)$:

$$\frac{1}{\Delta x^2}(\varphi_{i-1} - 2\varphi_i + \varphi_{i+1}) = -\frac{1}{\varepsilon\varepsilon_0}\rho_{q_{SAC}}L_i,\ i = 2, \ldots, N-1, \tag{26}$$

   and the system (23),(24),(26) becomes a system of linear equations. This system is solved for φ_i values utilizing *SciPy linalg.solve* routine [49].

(c) For each i, the obtained φ_i is compared to the corresponding $\varphi_{i(in)}$. If convergence within accepted relative tolerance (10^{-7}) is attained for every i, then the obtained φ_N and ρ_{qSAC} are used in Step 4. Otherwise, Step 3a is repeated with new $\varphi_{i(in,new)}$ which is assigned for each i as the arithmetic average of the just obtained solution φ_i and $\varphi_{i(in)}$ values from 100 most recent iterations of Step 3a (if $x < 100$ iterations are done by this point, then the earliest $\varphi_{i(in)}$ is included $100-x$ times for computing the average). Typically, convergence is attained within 10 seconds when running on one core of a *64-bit x86* CPU.

4. Calculate the proton concentration near the cellulose surface:

$$C_{H^+_{cell}} = \frac{\rho_{qSAC}}{F} \exp(-\frac{F}{RT}\varphi_N). \tag{27}$$

This is the value we use to judge if any hydrolytic activity can be expected from the diffuse layer.

5. Calculate the surface density of electrostatic potential energy on the cellulose surface:

$$W_{cell} = \varphi_N \sigma_{cell} = \varphi_N F \Gamma_{cell} \frac{C_{H^+_{cell}}}{K_c + C_{H^+_{cell}}}. \tag{28}$$

This value will be important for calculating the overall electrostatic potential energy in the system.

6. Use the algorithm Steps 3-5 to calculate $W_{cell(j)}$, $j = 1, \ldots, M$ values for several (typically $M = 20$) interplanar distances $d_{ip(j)}$ in the range from 0.5 nm to $r/\ 20$. The whole model is built around planar interacting surfaces, and trying to extrapolate the obtained data towards long distances from a spherical particle makes no sense. The Derjaguin approximation for the force of interaction between spheres has the same limitations [37]. We chose 5 % of the particle radius as the maximum interparticle distance that we account for.

7. This step estimates the electrostatic potential energy U_E of a spherical cellulose particle in the diffuse electrical layer. As a simplification, we assume that a cellulose particle interacts with one SAC particle, but this SAC-cellulose pair does not interact with any other solid particles in the reactor.

(a) We start from the state of contact with a spherical SAC particle. There is one point of contact, and the spheres are not deformed. Both particles have radius r_p. $U_{E(0)}$ is calculated by trapezoid-rule integration of W_{cell} along the particle surface according to Equation (29):

$$U_{E(0)} = \sum_{j=1}^{M} \frac{W_{cell(j-1)} + W_{cell(j)}}{2} s_j,\ W_{cell(0)} = 0, \tag{29}$$

where s_j is the area of the spherical zone of the corresponding segment (the concept is illustrated by Figure 2). The energy in the point where the spheres touch ($W_{cell(0)}$, the initial value for integration by Equation (29)) is considered zero, as there is no space for water, and so dissociation or protonation are not possible.

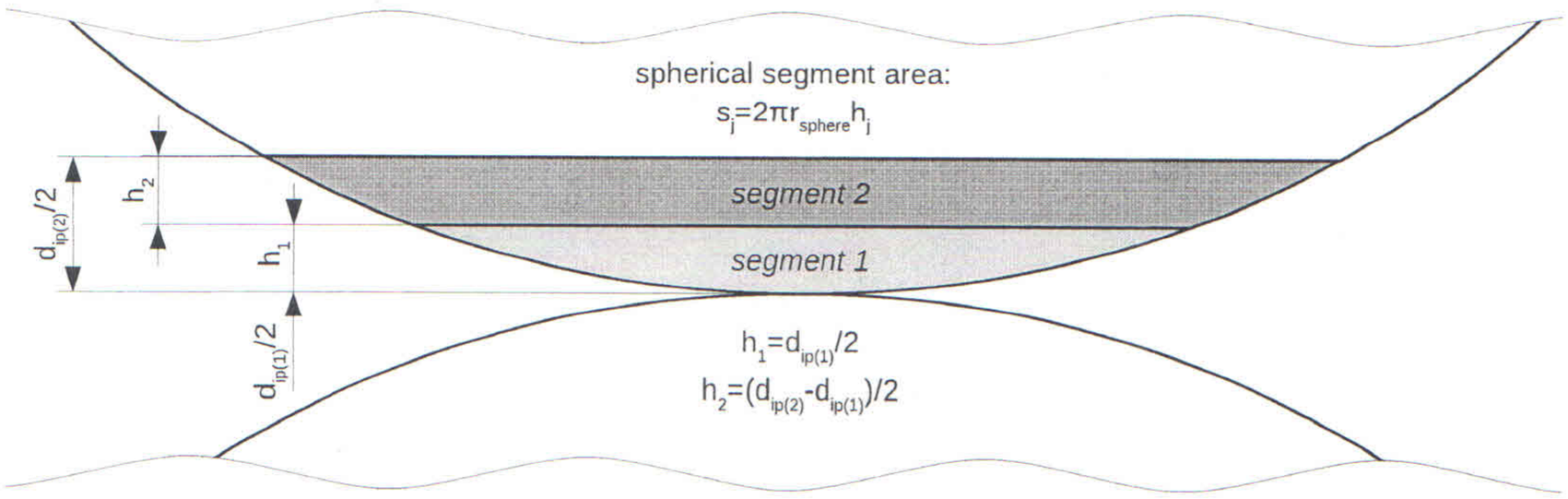

Figure 2: Schematic representation of discretization of the cellulose spherical particle for the calculation of the electrostatic potential energy in the state of contact with a spherical SAC particle. In this example, only the first two segments are shown.

(b) At nonzero distance between the particles, the potential energy is calculated by integration of the Derjaguin force (30) [37]:

$$F_{D(j)} = \pi r_p W_{cell(j)}, \tag{30}$$

$$U_{E(j)} = U_{E(0)} + \sum_{j=1}^{M} \frac{F_{D(j-1)} + F_{D(j)}}{2} (d_{ip(j)} - d_{ip(j-1)}),\ F_{D(0)} = F_{D(1)},\ d_{ip(0)} = 0, \tag{31}$$

here the meaning of d_{ip} is the distance between the nearest points of the two spheres. Since the Derjaguin force cannot be calculated at the point of contact, in this approximation we consider the force between the particles at their contact $F_{D(0)}$ to be equal to the force at the minimal accounted non-zero distance $F_{D(1)}$.

8. The calculated electrostatic potential energy U_E gains a physico-chemical meaning when transformed into the free energy value. To do so, we need to account for the entropy S_s of the solid particles, and this value can become quite large when the particle size decreases (which means an increase of the number of particles per unit mass). Stabilization of suspensions due to this effect when the dispersed phase becomes more finely divided is well known in colloid chemistry [34]. Finding exact thermochemical functions of the studied system is complicated and falls out of scope of the present paper. However, we can estimate how U_E and S_s change with particle size, which should be sufficient to provide qualitative trends related to the role of electrostatic attraction in cellulose hydrolysis.

S_s represents the part of entropy that depends on the number of particles in the reactor. All other factors contributing to entropy (bulk substance entropy) are considered to be independent of the particle size r_p and interparticle distance, and as such are disregarded in this approximation.

We will use statistical thermodynamics to estimate the entropy versus particle size. As an approximation, we consider that the solid particles behave like ideal gas, and that each particle's partition function z includes only the terms for translational z_{trans} and rotational z_{rot} motion. Within the ideal gas approximation, average energies of these two types of motion are equal, so $z_{trans} = z_{rot}$. Therefore, the thermodynamic parameters of interest can be expressed [50] as:

$$z = z_{trans}^2 = V^2 \left(\frac{2\pi m k_B T}{h^2} \right)^3, \tag{32}$$

$$A = -N k_B T \left(\ln(\frac{z}{N}) + 1 \right), \tag{33}$$

$$S_s = -\left(\frac{\partial A}{\partial T} \right)_V = N k_B \left(\ln \left(\frac{V^2}{N} \left(\frac{2\pi m k_B T}{h^2} \right)^3 \right) - 2 \right), \tag{34}$$

where V is the liquid volume (has little influence on the result within the practically interesting range of values, and is considered to be 10^{-3} m^3), m is mass of a particle, N is the number of particles, $k_B$is the Boltzmann constant, h is the Planck constant, and A is the Helmholtz free energy. We consider that in the reactor, there are N particles of SAC and N of cellulose, and all of them are spheres of equal radii. For convenience, we use N corresponding to one mole of glucose links ($C_6H_{10}O_5$, 162.14 g mol^{-1}) and an arbitrary r_p (which is varied in calculations). We also assume that they form pairs where one SAC particle interacts with one cellulose particle, but these pairs do not electrostatically interact with each other. In the state of particle contact as defined in the previous step, we consider that there are N solid particles, each having the combined mass of a SAC and a cellulose particle, and S_s is calculated for them. When there is no contact, S_s is calculated separately for SAC and for cellulose, and the resulting values are added together.

Finally, the estimated free energy of electrostatic interaction is defined as:

$$A_E = N U_E - T S_s. \tag{35}$$

Surface energy and free energies of the bulk substances are disregarded in this approximation because neither is assumed to depend on the interparticle distance. Indeed, when achieving the state of contact, the particles effectively coagulate rather than coalesce, and the total surface area (and consequentially, surface energy) remain practically unchanged.

Relative probability of finding a pair of interacting particles at a given distance between their closest points can be found by calculating $A_{E(j)}$ for this distance and applying the Boltzmann distribution:

$$p_j = \exp(-\frac{A_{E(j)}}{N k_B T}) \tag{36}$$

3 Results

Before the calculation results are discussed, we should remind that the model is based on several simplifications and approximations, and interpretation of the results should be limited to mostly qualitative or semi-quantitative conclusions.

3.1 Near-cellulose concentration of protons in the diffuse layer

Figure 3 shows the calculated dependence of near-cellulose proton concentration versus distance between the interacting surfaces for different catalyst properties. With strongly acidic functional groups, proton concentrations in the range 0.1–1 M are attained for interplanar distances up to a few nanometers. For comparison, the Scholler process of cellulose hydrolysis by dilute sulfuric acid [5] operates at proton concentrations around 0.1 M. However, quantitative comparison of hydrolysis rates based on the proton concentrations in a diffuse layer and in a homogeneous acid may be problematic: Apart from the limitations of our simplistic model, there is also the fact that the diffuse layer contains no dissolved acid anions, but homogeneous acids are known to form complexes with carbohydrates [5]. This phenomenon very likely plays a significant role in hydrolysis kinetics, similarly to how the patterns of specific catalysis by protons are broken by different substituted benzoic acids [32] (see Introduction). For now, we shall conclude that based on the proton concentration alone, it appears plausible that the electrical double layer of sulfonated SACs can make a significant contribution to the practically observed hydrolysis rates—but only if the electrostatic attraction and/or chemisorption can retain a cellulose particle in the very thin concentrated layer.

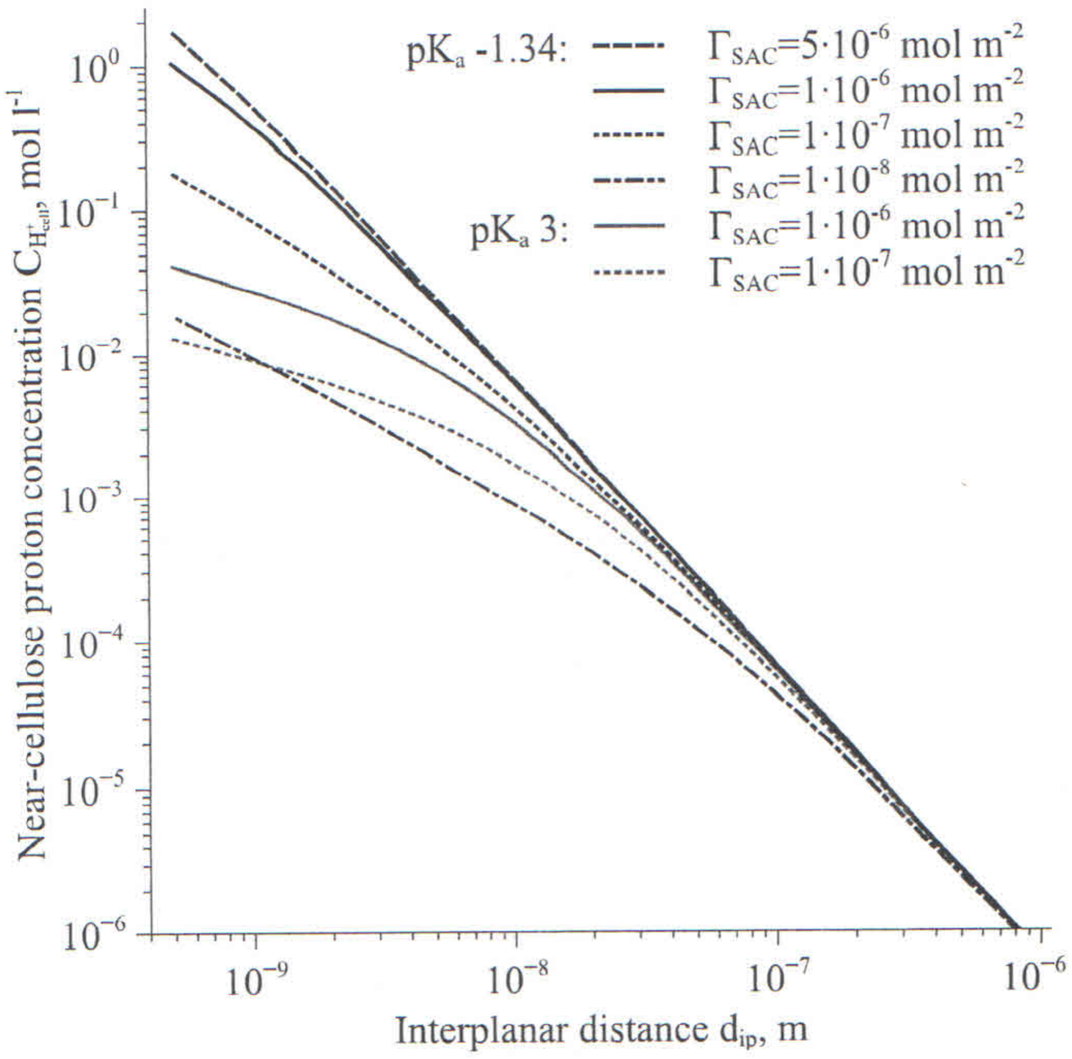

Figure 3: Dependence of near-cellulose proton concentration $C_{H^+_{cell}}$ versus interplanar distance d_{ip} for various catalyst acidity pK_a and catalyst acid group concentration Γ_{SAC} values. Temperature 453.15 K, water relative dielectric constant 38.6.

In the same range of distances (up to a few nanometers), the diffuse layer of weakly acidic SACs (i.e., oxidized carbons) exhibits proton concentrations that are lower by at least an order of magnitude when compared to strongly acidic SACs. Based solely on this criterion, the hydrolytic activity of oxidized carbons should be proportionally lower than that of strongly acidic SACs. However, in practice, this is typically not the case: the activity of oxidized carbons is comparable to that of sulfonated carbons [17, 51]. On the other hand, one case is known where an activated carbon catalyst (acid group count at 77 % of the sulfonated carbon used in the same study) resulted in the conversion of cellulose that was more or less equal to that in a blank run [9]. This will be analyzed in more detail in the Discussion section.

Interestingly, starting from the interplanar distance 50 nm, $C_{H^+_{cell}}$ becomes practically independent of the catalyst acid strength or functionalization density. Proton concentrations here (1 mM and below) seem insignificant in terms of catalyzing cellulose hydrolysis. However, this concentration may still be considerable in terms of cellulose protonation and interparticle attraction. This will be discussed in more detail in the net Subsection.

3.2 Electrostatic interaction energy

Figure 4a presents electrostatic potential energy U_E between one SAC particle and one cellulose particle; both particles are spheres of equal radius r_p. Interparticle distance $d_{ip} = 0$ corresponds to single-point contact between the spheres, non-zero d_{ip} values correspond to the distance between the two nearest points of the two spheres (one point on the SAC, one on the cellulose).

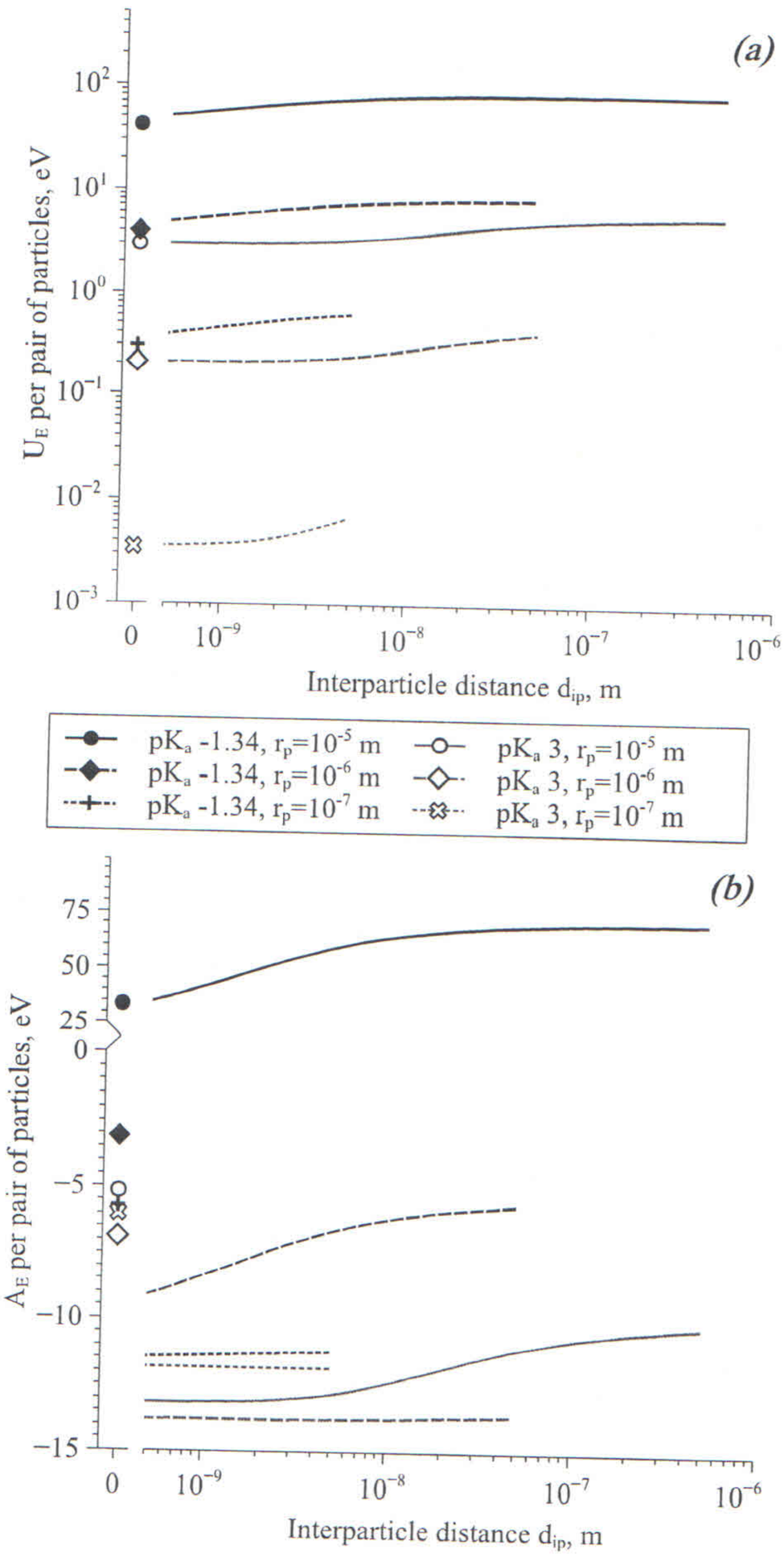

Figure 4: Estimated electrostatic potential energy U_E *(a)* and Helmholtz free energy A_E *(b)* of interaction between spherical SAC and cellulose particles, versus distance between the particles' nearest points d_{ip}. The energy values are given per one cellulose-SAC pair of interacting particles. Temperature 453.15 K ($k_BT = 0.039$ eV). $\Gamma_{SAC} = 10^{-6}$ mol m^{-2}. The number of cellulose particles in the reactor is assigned as $2.42{\cdot}10^{10}$, $2.42{\cdot}10^{13}$, and $2.42{\cdot}10^{16}$ for r_p 10^{-5}, 10^{-6}, and 10^{-7} m respectively (corresponding to the total of 162.14 g cellulose, or 1 mol of glucose links). For calculation details, please refer to Subsection 2.3 Steps 7-8.

It can be seen that depending on SAC acidity and particle size, U_E per particle can vary by several orders of magnitude (Figure 4a). This energy spans from a few meV for weakly acidic SAC and $r_p = 10^{-7}$ m to dozens of eV for strongly acidic catalyst and $r_p = 10^{-5}$ m. More importantly, the energy gain resulting from separation of the interacting particles to the maximum distance $\Delta U_{E(sep)}$ has the same order of magnitude as the energy at contact $U_{E(d_{ip}=0)}$. Comparing $\Delta U_{E(sep)}$ with thermal motion energy (k_BT) provides the first approximation of whether the particles tend to attract and adhere to each other via electrostatic

force. For example, for weak acid and $r_p = 10^{-7}$ m, $\Delta U_{E(sep)} \sim 1$ meV which is considerably lower than $k_B T = 39$ meV, and thus from Boltzmann distribution it follows that separation of the particles is insignificantly less probable than the state of contact. In other words, in this case, the electrostatic attraction has negligible effect on the two particles' relative position. In this case, adherence of the particles can only be achieved through chemisorption when the particles forcibly collide due to stirring (or, less likely, collide due to Brownian motion). Although the adsorption energy is considerable ($\Delta G_{ads} \approx -120$ meV per glucose link [31]), chemisorption of cellulose onto SAC appears to be a chancy process, as will be shown in the Discussion section. By contrast, with strong acid and large particles, $\Delta U_{E(sep)}$ can attain ~ 10 eV which means that adherence is greatly favored over separation of the particles.

An important thing worth noting here is that electrostatic attraction between the particles manifests even at distance, unlike chemisorption that requires direct contact. This means that electrostatic attraction may be a facilitating factor in establishing chemisorption, by keeping the particles close to each other until chemisorption eventually takes place. Furthermore, if strong acid groups are present on the SAC, then chemisorption is not even necessary for hydrolysis because electrostatic attraction will reliably keep the cellulose within the high concentration zone of the diffuse layer of protons (Figure 3).

At this point, it is important to remind that the analysis offered in the previous paragraph may not scale well towards numerous particles, even if they form independent pairs of one SAC particle and one cellulose particle. Growing number of particles leads to higher entropy. In colloid chemistry, it is known that suspensions may become stable when particles become sufficiently small and their entropy per unit mass becomes high enough to overcome higher surface energy of the finely dispersed state. Application of this trend to our model means that when the size of solid particles becomes small enough, their high entropy may counteract the electrostatic potential energy, and attraction between the particles would cease to be.

We made an attempt to estimate the entropy versus particle count. The resulting electrostatic free energy (Subsection 2.3 Step 8) is presented in Figure 4b. The abrupt change of A_E upon particle contact is due to the simplicity of entropy approximation: A cellulose particle and a SAC particle are treated as monoatomic ideal gas particles until the moment of contact, at which point the number of particles in the system is halved. I.e., the interaction force between the particles is ignored altogether when estimating the entropy. So, the calculated free energy illustrates only a qualitative trend concerning the influence of particle size on the probability of electrostatic adherence. It can be seen that in case of strongly acidic SAC and $r_p = 10^{-5}$ m, the A_E dependence versus d_{ip} is practically indistinguishable from the corresponding dependence of U_E (Figure 4a). In other cases, the state of separation becomes more favorable by ~ 10 eV per one pair of interacting particles. This would make interparticle adhesion by electric force practically impossible even though U_E alone greatly favors attraction (e.g., $pK_a = 3$, $r_p = 10^{-5}$ m).

Assuming that the Boltzmann distribution applies to the calculated free energies, the relative probability of finding the two particles at a given distance from each other can be plotted (Figure 5). The tendency for electrostatic attraction of cellulose to large particles of a strong solid acid is clear. On the other hand, as the particles become smaller and the acid becomes weaker, there is a trend towards equiprobability of all interparticle distances. In other words, electrostatic factor can be expected to become negligible in determining relative positions of solid particles if the solid acid is weak and the interacting particles are sufficiently finely divided (e.g., due to excessive milling or disintegration of particles in the reactor).

4 Discussion

In this section, we analyze how our calculations concerning the electrical double layer in the system water-SAC-cellulose can explain various experimental results described in literature.

4.1 Catalysts with pure sulfonic functionalization

Successful hydrolysis of cellulose with Amberlyst-15 sulfonic ion exchange resin was reported [9, 11]. A peculiar feature of this catalyst is that despite substantial cellulose conversion, glucose can comprise as little as a half of the hydrolysis products (Table 1). The non-glucose portion of the conversion products was identified as predominantly oligosaccharides [11]. From our model's point of view, this result has an explanation. As demonstrated by Figures 4-5, a strong solid acid can be feasibly expected to attract cellulose, pulling the solid substrate into the thin diffuse layer with high proton concentration (Figure 3) which facilitates fast conversion of the solid substrate. Hydrolysis of cellulose is catalyzed by the protons of the diffuse layer; polysaccharide molecules are hydrolyzed at random locations along their length, which leads to formation of oligosaccharides. However, the conditions do not favor further hydrolysis of the latter. Firstly, Amberlyst-15 does not chemisorb sugars [10]. Secondly, even if the oligosaccharide molecules are sufficiently protonated to experience attraction to the SAC polyanion, the entropic factor will

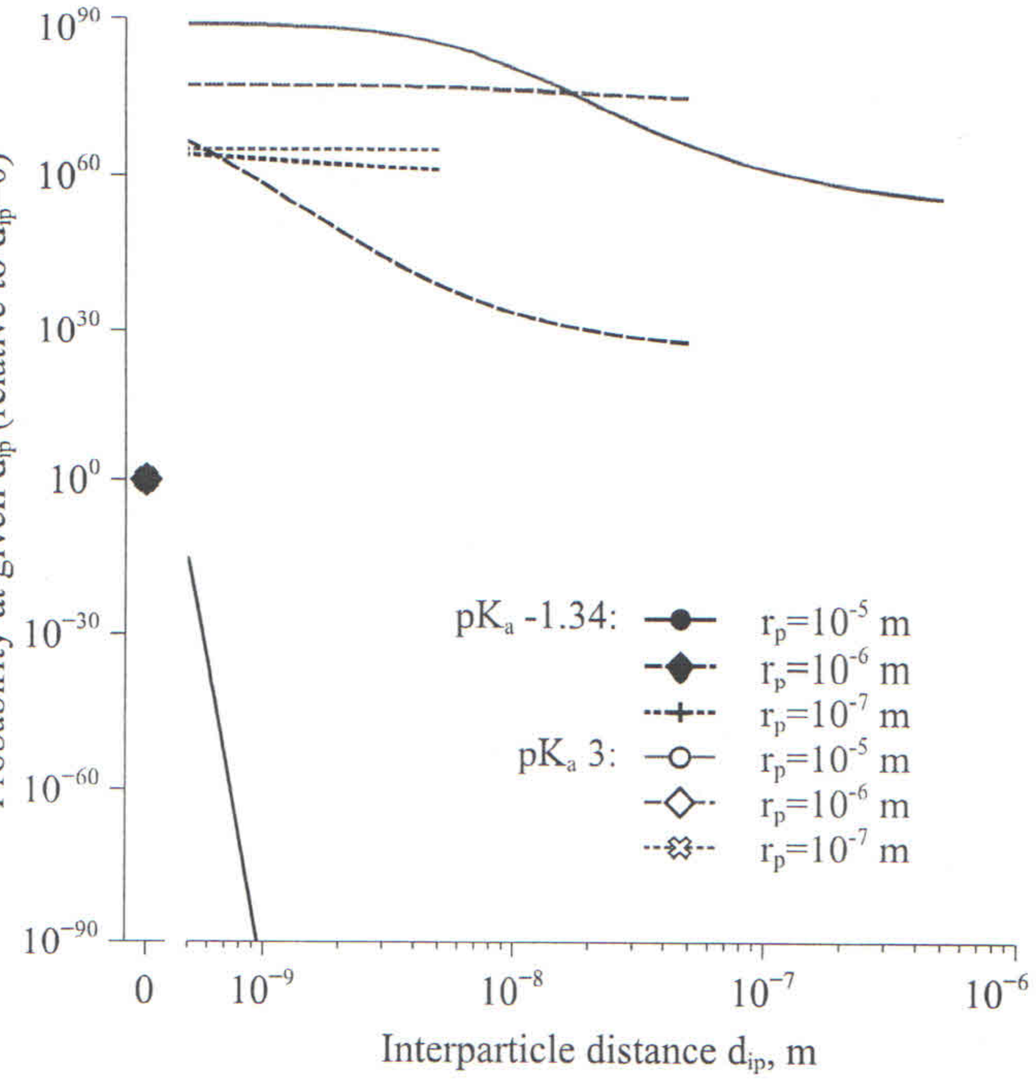

Figure 5: Relative probability of finding a SAC-cellulose pair of spherical particles at distance d_{ip} from each other. For each particle radius r_p and SAC acidity pK_a, the probability is relative to that of finding the same pair of particles at $d_{ip} = 0$. The probabilities are based on Boltzmann distribution of the electrostatic free energy A_E values as presented in Figure 4b.

overpower this attraction anyway. Growing number of particles is predicted to negate electrostatic attraction of solid cellulose to the catalyst (Fig. 4b), and oligosaccharide molecules quickly become very numerous during hydrolysis (e.g., in a cited experiment [11], assuming 10 glucose links per oligosaccharide molecule, 15 % yield of oligosaccharides from 50 mg of cellulose would correspond to $2.8 \cdot 10^{18}$ molecules, which outnumbers the largest number of particles we tried accounting for in 4b). This means that the oligosaccharides are uniformly distributed in space, and can only undergo hydrolysis when they diffuse into the concentrated proton layer. But this layer is very thin (Figure 3): at the layer thickness 3 nm, catalyst loading 50 mg, volume of water 5 mL, and assuming that catalyst particles have radius 1 μm, the concentrated layer occupies approximately 0.08 ‰ of the liquid volume. Therefore, hydrolysis of oligosaccharides is not fast and they tend to accumulate in the reactor.

Table 1: Literature data on cellulose hydrolysis with Amberlyst-15.

Temperature, K	Duration, h	Stirring	Cellulose conversion, %	Glucose yield, % of initial cellulose	Reference
423	24	22 rpm	31	26	[9]
423	24	vigorous	52	28	[11]
373	7	n/a	0	0	[10]

Similar cellulose conversion and glucose yield were observed under similar conditions when using an SBA-15 mesoporous silica material modified with sulfonic groups [22]. This suggests that the catalyst structure (reticular Amberlyst-15 or mesoporous SBA-15) has no significant influence on hydrolysis outcome with SACs bearing sulfonic groups but no organic acid sites. This would be expected when the catalytic reaction takes place in the diffuse layer and does not directly involve the SAC surface or internal structure at all. So, this observation concerning the lack of catalyst structure influence on the hydrolysis process supports the hypothesis about the diffuse layer as the reaction zone.

Amberlyst-15 exhibits no hydrolytic activity at 373 K [10]. As mentioned, this catalyst has no chemisorption affinity for carbohydrates [10], so there are no obvious preconditions for direct chemical solid-to-solid interactions. As for the diffuse proton layer, the temperature 373 K is not sufficient for hydrolysis by dilute acids (even removal of hemicellulose from wood requires at least 400 K [5]).

Despite weak agitation of the reaction medium in [9], cellulose conversion is still comparable to the experiment with more intense stirring [11]. This supports the hypothesis about strong electrostatic attraction of cellulose to strong solid acids. Evidently, the attraction is strong enough to eventually cause adhesion even if the solid particles do not frequently forcibly collide due to

stirring. As will be shown in the next Subsection, the situation with weak solid acids appears to be quite different.

4.2 Oxidized and oxidized-sulfonated carbons

Unlike purely sulfonic catalysts [10], oxidized carbons strongly chemisorb carbohydrates [31], which is likely caused by synergy between neighboring carboxylic and hydroxylic groups [32]. On the other hand, these acidic groups are too weak to form a substantial diffuse proton layer in water (Figure 3); the prospects of electrostatic attraction are not promising too (Figures 4b,5). However, hydrolysis of cellulose with such catalysts is typically quite effective (Table 2). In fact, oxidized carbons were reported to exceed the activity of sulfonated carbons when the latter contain lower amounts of organic acidic groups (e.g., in Table 2, AC-NO_3 versus AC-SO_3H-150, or C-O versus C-S150). Evidently, far higher hydrolytic turnover rate can be attained by organic acid sites via chemisorption than by sulfonic sites acting via the diffuse electrical layer.

Table 2: Some examples of literature data on hydrolysis of cellulose with oxidized and oxidized-sulfonated carbons.

Catalyst designation	Sulfonic groups content, mmol g^{-1}	Total acid groups content, mmol g^{-1}	Temperature, K	Duration, h	Stir rate, rpm	Cellulose conversion, %	Glucose yield, % of initial cellulose	Refe-rence
none (blank run)	n/a	n/a	423	24	22	13	3	[9]
AC	0	1.25	423	24	22	10	9	[9]
AC-SO_3H	0.44	1.63	423	24	22	45	42	[9]
AC-NO_3	0.02	1.49	423	24	100	31.5	9.7	[52]
AC-SO_3H-150	0.19	0.80	423	24	100	25.1	7.1	[52]
AC-N-SO_3H-200	0.24	1.03	423	24	100	64.3	56.1	[52]
C-O	below detection	0.28	453	7	1500	60.1	27.4	[51]
C-S150	≈0.17[a]	0.32	453	7	1500	52.1	23.5	[51]
C-S200	≈0.11[b]	0.40	453	7	1500	65.3	18.9	[51]
carbon material	1.9	4.3	373	3	n/a	64	4	[10]

[a] inferred from XPS analyses of different catalyst samples
[b] see Footnote *a*

There exists one peculiar case (catalyst AC [9]), where conversion of cellulose with an activated carbon catalyst was more or less the same as in a blank run, i.e., the catalyst had no effect on the solid substrate. Still, the oligosaccharides formed due to destruction of cellulose with hot water and/or impurities were effectively hydrolyzed into glucose, which shows that the functional groups necessary for carbohydrate hydrolysis were present on the catalyst. In our opinion, there is an explanation of this phenomenon from our model's point of view. The distinguishing feature of this unsuccessful experiment with activated carbon is weak agitation of the reaction medium. As was frequently emphasized in this paper, no notable electrostatic attraction is expected between weakly acidic SACs and cellulose, therefore the only way to establish direct solid-to-solid contact necessary for hydrolysis via chemisorption would be by using strong agitation to ensure frequent collisions between the particles. The outcome of the cited experiment with the AC catalyst [9] appears to support this hypothesis. By contrast, strong agitation is not necessary for high cellulose conversion over Amberlyst-15 (Table 1) since sufficient adhesion to cellulose is maintained by the strong electrostatic attraction predicted by our model.

Combining sulfonic and organic acid groups in one catalyst allows combining the benefits of both functionalization types. Organic acid groups have high turnover rate when adsorption is achieved. Strong acid groups ensure reliable attraction of the interacting solids, and this facilitates adsorption of cellulose on the catalyst because the interacting particles do not need to wait for a collision (due to Brownian motion or agitation) to have a chance to chemisorb. And once a collision takes place, it is not guaranteed to result in chemisorption because—like any chemical reaction—it has to overcome a certain activation barrier. Electrostatic attraction due to the electrical double layer can constantly keep the two solids in contact, which gives more time for chemisorption to occur. The idea about predominantly supportive role of the sulfonic groups in combined catalysts is corroborated by the fact that the apparent activation energy of cellulose hydrolysis over a catalyst with both types of acid groups (110 kJ mol^{-1}) [10] is similar to that of hydrolysis with benzoic acid and its derivatives (110-120 kJ mol^{-1}) [32], rather than with sulfuric acid (170 kJ mol^{-1}) [10]. This suggests that carboxylic groups are involved in the chemical reaction step of the hydrolysis process to

much greater extent than sulfonic groups. The described roles of sulfonic and organic groups in the catalysis process (coordination of cellulose and the actual hydrolysis chemical reaction, respectively) appear to be a reversal of what was theorized in [10].

So, although strongly acidic groups make only a modest contribution in terms of acid catalytic action when compared to synergistic carboxylic-phenolic ensembles, the former play an important role in establishing chemisorption that is necessary for the latter to work. This is well illustrated by comparing the adsorption properties of different catalysts (Table 3). The carbon material with combined sulfonic-organic functionalization is the only type of catalyst that readily adheres to solid cellulose, and does this strongly enough to withstand ultrasonic cleaning [10]. Such difference in affinity for cellulose appears to not have strong effect on hydrolysis rate at high temperature (453 K, compare C-O, C-S150, C-S200 in Table 2), but the synergy becomes more pronounced when the temperature is lowered by 30 K (compare AC-NO_3, AC-SO_3H-150, AC-N-SO_3H-200 in Table 2). This may be attributable to the entropic factor that increases with temperature (Equations (34)-(35)) and counteracts the electrostatic attraction generated by the sulfonic groups (as described in Subsection 3.2). A combined catalyst was reported to perform well even at 373 K [10]—the temperature that ordinarily requires concentrated acids to enable cellulose hydrolysis. However, this unusually high activity at low temperature may be attributed to some different, as yet unidentified effects related the exceptionally high acid group concentration in this catalyst.

Table 3: Comparison of carbohydrate adsorption on different solid acids.

Catalyst designation	Sulfonic groups content, mmol g^{-1}	Total acid groups content, mmol g^{-1}	Adsorption of soluble sugars	Adhesion to cellulose	Reference
K26	n/a[a]	1.4	yes	no	[31]
Amberlyst-15	4.8	4.8	no	no[b]	[10]
carbon material	1.9	4.3	yes	yes[c]	[10]

[a] not explicitly sulfonated
[b] after ultrasonic cleaning
[c] see Footnote *b*

5 Conclusion

For the first time, the role of electrical double layer in hydrolysis of cellulose over insoluble solid acids in aqueous media was studied. Although the proposed model of interaction between solid acid catalysts and cellulose mediated by electrical double layer is based on several approximations and simplifications, our calculations harmoniously combine with literature data about chemisorption of carbohydrates. As the result, a variety of experimental data from literature can be adequately explained at least on qualitative level.

Protonation of cellulose by the diffuse proton layer of solid catalysts with strong (sulfonic) acid groups causes electrostatic attraction of the solid carbohydrate to the catalyst. This ensures that close contact between the two solids is constantly maintained. So, cellulose is constantly immersed in thin but concentrated diffuse proton layer where hydrolysis takes place. This electrostatic attraction also facilitates establishing chemisorption with catalysts that bear organic (carboxylic and phenolic) acid groups. Organic acid groups are too weak to create a concentrated proton layer and to cause appreciable attraction; but once chemisorption is established (by mechanical collision or by attraction due to sulfonic groups), they exhibit higher hydrolytic activity than sulfonic groups. The influence of electrostatic attraction between the catalyst and the cellulose is believed to decrease when temperature increases and/or solid particles become smaller.

Still, the proposed model is too simplistic to account for many variables, e.g., textural characteristics of catalysts (porosity, specific surface area). There are also not enough data to quantitatively predict the hydrolytic activity of such an unusual acid as a cloud of protons whose space charge is not compensated by homogeneous acid anions. More detailed calculation models and more experimental data with different sulfonated catalysts (or with otherwise strong Brønsted acidic functionalization) are necessary for the further study of this phenomenon.

References

[1] Avelino Corma, Sara Iborra, and Alexandra Velty. Chemical routes for the transformation of biomass into chemicals. *Chemical Reviews*, 107(6):2411–2502, 2007. PMID: 17535020.

[2] Sergey Dmitrievich Varfolomeev, Ilya Iosifovich Moiseev, and Boris Fedorovich Myasoedov. Energy carriers from renewable raw materials. *Herald of the Russian Academy of Science*, 79(7):595–604, 2009. In Russ.

[3] David Martin Alonso, Jesse Q. Bond, and James A. Dumesic. Catalytic conversion of biomass to biofuels. *Green Chem.*, 12:1493–1513, 2010.

[4] Roger A. Sheldon. Green and sustainable manufacture of chemicals from biomass: state of the art. *Green Chem.*, 16:950–963, 2014.

[5] Liang-tseng Fan, Mahendra Moreshwar Gharpuray, and Yong-Hyun Lee. *Acid Hydrolysis of Cellulose*, pages 121–148. Springer Berlin Heidelberg, Berlin, Heidelberg, 1987.

[6] Bin Yang, Ziyu Dai, Shi-You Ding, and Charles E Wyman. Enzymatic hydrolysis of cellulosic biomass. *Biofuels*, 2(4):421–449, 2011.

[7] Kosuke Kuroda, Kyohei Miyamura, Heri Satria, Kenji Takada, Kazuaki Ninomiya, and Kenji Takahashi. Hydrolysis of cellulose using an acidic and hydrophobic ionic liquid and subsequent separation of glucose aqueous solution from the ionic liquid and 5-(hydroxymethyl)furfural. *ACS Sustainable Chemistry & Engineering*, 4(6):3352–3356, 2016.

[8] R. M. Wahlstrom and A. Suurnakki. Enzymatic hydrolysis of lignocellulosic polysaccharides in the presence of ionic liquids. *Green Chem.*, 17:694–714, 2015.

[9] Ayumu Onda, Takafumi Ochi, and Kazumichi Yanagisawa. Selective hydrolysis of cellulose into glucose over solid acid catalysts. *Green Chem.*, 10:1033–1037, 2008.

[10] Satoshi Suganuma, Kiyotaka Nakajima, Masaaki Kitano, Daizo Yamaguchi, Hideki Kato, Shigenobu Hayashi, and Michikazu Hara. Hydrolysis of cellulose by amorphous carbon bearing so3h, cooh, and oh groups. *Journal of the American Chemical Society*, 130(38):12787–12793, 2008. PMID: 18759399.

[11] Stijn Van de Vyver, Li Peng, Jan Geboers, Hans Schepers, Filip de Clippel, Cedric J. Gommes, Bart Goderis, Pierre A. Jacobs, and Bert F. Sels. Sulfonated silica/carbon nanocomposites as novel catalysts for hydrolysis of cellulose to glucose. *Green Chem.*, 12:1560–1563, 2010.

[12] Deepak Verma, Rashmi Tiwari, and Anil Kumar Sinha. Depolymerization of cellulosic feedstocks using magnetically separable functionalized graphene oxide. *RSC Adv.*, 3:13265–13272, 2013.

[13] Mizuho Yabushita, Hirokazu Kobayashi, and Atsushi Fukuoka. Catalytic transformation of cellulose into platform chemicals. *Applied Catalysis B: Environmental*, 145:1 – 9, 2014.

[14] Hirokazu Kobayashi, Yuto Hosaka, Kenji Hara, Bo Feng, Yoshihiko Hirosaki, and Atsushi Fukuoka. Control of selectivity, activity and durability of simple supported nickel catalysts for hydrolytic hydrogenation of cellulose. *Green Chem.*, 16:637–644, 2014.

[15] Abhijit Shrotri, Hirokazu Kobayashi, and Atsushi Fukuoka. Cellulose depolymerization over heterogeneous catalysts. *Accounts of Chemical Research*, 51(3):761–768, 2018.

[16] Maksim Tyufekchiev, Pu Duan, Klaus Schmidt-Rohr, Sergio Granados Focil, Michael T. Timko, and Marion H. Emmert. Cellulase-inspired solid acids for cellulose hydrolysis: Structural explanations for high catalytic activity. *ACS Catalysis*, 8:1464–1468, 2018.

[17] Nikolai V. Gromov, Artem B. Ayupov, Cyril Aymonier, Vladimir E. Agabekov, and Oxana P. Taran. Development of solid acid catalysts based on sibunit carbon material for cellulose transformation into 5-hydroxymethilfurfural. *Journal of Siberian Federal University. Chemistry*, 7(4):597–609, 2014. in Russ.

[18] Yao-Bing Huang and Yao Fu. Hydrolysis of cellulose to glucose by solid acid catalysts. *Green Chem.*, 15:1095–1111, 2013.

[19] Abhijit Shrotri, Hirokazu Kobayashi, and Atsushi Fukuoka. Air oxidation of activated carbon to synthesize a biomimetic catalyst for hydrolysis of cellulose. *ChemSusChem*, 9(11):1299–1303, 2016.

[20] Hirokazu Kobayashi and Atsushi Fukuoka. Development of solid catalyst–solid substrate reactions for efficient utilization of biomass. *Bulletin of the Chemical Society of Japan*, 91(1):29–43, 2018.

[21] Olga V. Yatsenkova, Anna I. Chudina, Svetlana A. Kozlova, Andrei M. Skripnikov, Oxana P. Taran, Nikolai V. Chesnokov, and Boris N. Kuznetsov. Influence of the nature of acid solid catalysts on their activity in the hydrolysis of sucrose and cellulose. *Journal of Siberian Federal University. Chemistry*, 7(2):226–235, 2014.

[22] B. N. Kuznetsov, N. V. Chesnokov, O. V. Yatsenkova, V. I. Sharypov, N. V. Garyntseva, N. M. Ivanchenko, and V. A. Yakovlev. Green catalytic valorization of hardwood biomass into valuable chemicals with the use of solid catalysts. *Wood Science and Technology*, (5), 2017. Online only.

[23] Daizo Yamaguchi, Masaaki Kitano, Satoshi Suganuma, Kiyotaka Nakajima, Hideki Kato, and Michikazu Hara. Hydrolysis of cellulose by a solid acid catalyst under optimal reaction conditions. *The Journal of Physical Chemistry C*, 113(8):3181–3188, 2009.

[24] Valery E. Tarabanko, Marina A. Smirnova, Mikhail Yu. Chernyak, Alexander A. Kondrasenko, and Nikolay V. Tarabanko. The nature and mechanism of selectivity decrease of the acid-catalyzed fructose conversion with increasing the carbohydrate concentration. *Journal of Siberian Federal University. Chemistry*, 8(1):6–18, 2015.

[25] Ben F.M. Kuster. The influence of water concentration on the dehydration of d-fructose. *Carbohydrate Research*, 54(2):177 – 183, 1977.

[26] David W. Brown, Arthur J. Floyd, Richard G. Kinsman, and Yusuf Roshanhyphen;Ali. Dehydration reactions of fructose in non-aqueous media. *Journal of Chemical Technology and Biotechnology*, 32(7):920–924, 1982.

[27] Valery E. Tarabanko, Marina A. Smirnova, Yulia V. Chelbina, and Mikhail Yu. Chernyak. The low-temperature synthesis of 5-hydroxymethylfurfural. *Khimia Rastitel'nogo Syr'ya*, (1):87–92, 2011. in Russ.

[28] Haile Cai, Changzhi Li, Aiqin Wang, Guoliang Xu, and Tao Zhang. Zeolite-promoted hydrolysis of cellulose in ionic liquid, insight into the mutual behavior of zeolite, cellulose and ionic liquid. *Applied Catalysis B: Environmental*, 123-124:333 – 338, 2012.

[29] Oz M. Gazit and Alexander Katz. Understanding the role of defect sites in glucan hydrolysis on surfaces. *Journal of the American Chemical Society*, 135(11):4398–4402, 2013.

[30] Oz M. Gazit, Alexandre Charmot, and Alexander Katz. Grafted cellulose strands on the surface of silica: effect of environment on reactivity. *Chemical Communications*, 47:376–378, 2011.

[31] Mizuho Yabushita, Hirokazu Kobayashi, Jun-ya Hasegawa, Kenji Hara, and Atsushi Fukuoka. Entropically favored adsorption of cellulosic molecules onto carbon materials through hydrophobic functionalities. *ChemSusChem*, 7(5):1443–1450, 2014.

[32] Hirokazu Kobayashi, Mizuho Yabushita, Jun-ya Hasegawa, and Atsushi Fukuoka. Synergy of vicinal oxygenated groups of catalysts for hydrolysis of cellulosic molecules. *The Journal of Physical Chemistry C*, 119(36):20993–20999, 2015.

[33] Roger Parsons. *Trends in Interfacial Electrochemistry. NATO ASI Series (Series C: Mathematical and Physical Sciences)*, volume 179, chapter Models of the Electrical Double Layer, pages 373–385. Springer Netherlands, Dordrecht, 1986.

[34] Yu. G. Frolov. *Study course in colloid chemistry. Surface phenomena and dispersed system.* Khimiya, Moscow, 1982. In Russ.

[35] Itamar Borukhov, David Andelman, Regis Borrega, Michel Cloitre, Ludwik Leibler, and Henri Orland. Polyelectrolyte titration: Theory and experiment. *The Journal of Physical Chemistry B*, 104(47):11027–11034, 2000.

[36] Rong Dong, Manfred Lindau, and Christopher K. Ober. Dissociation behavior of weak polyelectrolyte brushes on a planar surface. *Langmuir*, 25(8):4774–4779, 2009. PMID: 19243153.

[37] Boris Derjaguin. Untersuchungen ueber die reibung und adhaesion, iv. *Kolloid-Zeitschrift*, 69(2):155–164, Nov 1934.

[38] Johannes Lutzenkirchen, Tajana Preocanin, Davor Kovacevic, Vladislav Tomisic, Lars Lovgren, and Nikola Kallay. Potentiometric titrations as a tool for surface charge determination. *Croatica Chemica Acta*, 85(4):391–417, 2012.

[39] V. V. Sydorchuk, Svitlana V. Khalameida, O. I. Poddubnaya, M. M. Tsyba, and Alexander M. Puziy. Cation-containing active carbons as photocatalysts for dyes degradation. *Chemistry, Physics and Technology of Surface*, 8(4):422–431, 12 2017.

[40] E. P. Serjeant and B. Dempsey, editors. *Ionisation constants of organic acids in aqueous solution*. Number 23 in IUPAC chemical data series. Pergamon Press, New York, 1979.

[41] Michael B. Smith and Jerry March. *March's Advanced Organic Chemistry: Reactions, Mechanisms, and Structure*. Wiley, USA, 6 edition, 2007. 2374 pages.

[42] Charles Aloysius Meyer, American Society of Mechanical Engineers, and ASME Research Committee on Properties of Steam. *Thermodynamic and transport properties of steam: comprising tables and charts for steam and water calculated using The 1967 IFC formulation for industrial use, in conformity with the 1963 International skeleton tables as adopted by the Sixth International Conference on the Properties of Steam*, volume 1. American Society of Mechanical Engineers, New York, 6 edition, 1993. 436 pages.

[43] Hans-Jurgen Butt, Karlheinz Graf, and Michael Kappl. *Physics and Chemistry of Interfaces*, chapter The Electric Double Layer, pages 42–56. Wiley-Blackwell, 2 edition, 2004.

[44] Raymond A. Serway and John W. Jewett. *Physics for Scientists and Engineers with Modern Physics*. Cengage Learning, USA, 9 edition, 2003. 1616 pages.

[45] Yoshiharu Nishiyama, Junji Sugiyama, Henri Chanzy, and Paul Langan. Crystal structure and hydrogen bonding system in cellulose i-alpha from synchrotron x-ray and neutron fiber diffraction. *Journal of the American Chemical Society*, 125(47):14300–14306, 2003. PMID: 14624578.

[46] Wojciech Dabrowski, Marta Spaczynska, and R. Ian Mackie. A model to predict granular activated carbon backwash curves. *Clean Soil, Air, Water*, 36(1):103–110, 2008.

[47] P. H. Hermans and D. Vermaas. Density of cellulose fibers. i. introduction and experiments on the penetration of liquids into dry cellulose. *Journal of Polymer Science*, 1(3):149–155, 1946.

[48] Joe D. Hoffman. *Numerical Methods for Engineers and Scientists*, chapter One-Dimensional Boundary-Value Ordinary Differential Equations, pages 435–500. Marcel Dekker Inc., New York, 2 edition, 2001.

[49] Eric Jones, Travis Oliphant, Pearu Peterson, et al. Scipy: Open source scientific tools for python, 2001–. Online; accessed 6 Nov 2018.

[50] N. M. Bazhin, V. A. Ivanchenko, and V. N. Parmon. *Thermodynamic for chemists*. Khimiya, Moscow, 2000. In Russ.

[51] Nikolay V. Gromov, Tatiana B. Medvedeva, Oxana P. Taran, Andrey V. Bukhtiyarov, Cyril Aymonier, Igor P. Prosvirin, and Valentin N. Parmon. Hydrothermal solubilization-hydrolysis-dehydration of cellulose to glucose and 5-hydroxymethylfurfural over solid acid carbon catalysts. *Topics in Catalysis*, page 14, Sep 2018. Online-only.

[52] Jifeng Pang, Aiqin Wang, Mingyuan Zheng, and Tao Zhang. Hydrolysis of cellulose into glucose over carbons sulfonated at elevated temperatures. *Chem. Commun.*, 46:6935–6937, 2010.

Written with LyX, free document processor.

Vector graphics made with LibreOffice Draw, part of the free office suite.

Plots made with Veusz, free graphing tool.